yo, **1994**, p 359.
18. Shiomi, H.; Tanabe, K.; Nishibayashi, Y.; Fujimori, N. *Jpn. J. Appl. Phys.* **1990**, *29*, 34.
19. Schauer, S. N.; Flemish, J. R.; Wittstruck, R.; Landstrass, M. I.; Plano, M. A. *Appl. Phys. Lett.* **1994**, *64*, 1094.
20. Flemish, J. R.; Schauer, S. N.; Wittstruck, R. Landstrass, M. I.; Plano, M. A. *Diam. Relat. Mater.* **1994**, *3*, 672.
21. Dannefaer, S.; Zhu, W.; Bretagnon, T.; Kerr, D. *Phys. Rev. B* **1996**, *53*, 1979.
22. Hoffmann, R. *J. Chem. Phys.* **1963**, *39*, 1397.
23. Whangbo, M.-H.; Hoffmann, R. *J. Am. Chem. Soc.* **1978**, *100*, 6093.
24. Whangbo, M.-H.; Hoffmann, R.; Woodward, R. B. *Proc. R. Soc. London* A **1979**, *366*, 23.
25. Anderson, A. B.; Grantscharova, E. J.; Angus, J. C. *Phys. Rev. B* **1996**, *54*, 14341.
26. Ammeter, J. H.; Bürgi, H. B.; Thibeault, J. C.; Hoffmann, R. *J. Am. Chem. Soc.* **1978**, *100*, 3686.
27. Hoffmann, R. *Solids and Surfaces: A Chemist's View of Bonding in Extended Structures*; VCH; New York, **1988.**
28. Messmer R. P.; Watkins, G. D. *Phys. Rev. B* **1973**, *7*, 2568.
29. Mainwood, A. *J. Phys. C: Solid State Phys.* **1979**, *12*, 2543.
30. Sahoo, N.; Mishra, K. C.; van Rossum, M.; Dass, T. P. *Hyperfine Interact.* **1987**, *35*, 701.
31. Briddon, P. R.; Heggie, M. I.; Jones, R. in *New Diamond Science and Technology*, Messier, R.; Glass, J. T.; Butler, J. E.; Roy, R. (eds.), Pittsburgh, **1991**, p 63.
32. Erwin, S. C.; Pickett, W. E. *Phys. Rev. B* **1990**, *42*, 11056.
33. Cao, G. Z.; Driessen, F. A. J. M.; Bauhuis, G. J.; Giling, L. J.; Alkemade, P. F. A. *J. Appl. Phys.* **1995**, *78*, 3125.
34. Cao, G. Z.; van Enckevort, W. J. P.; Giling, L. J.; de Kruif, R. C. M. *Appl. Phys. Lett.* **1995**, *66*, 688.
35. Cao, G. Z.; Giling, L. J.; Alkemade, P. F. A. *Diam. Relat. Mater.* **1995**, *4*, 775.
36. Anderson, A. B.; Kostadinov, L. N. *J. Appl. Phys.* **1997**, *81*, 264.
37. Clark, C. D.; Dean, P. J.; Harris, P. V. *Proc. R. Soc.* London A **1964**, *277*, 312.
38. *Tables of Parameters for Extended Hückel Calculations*; collected by Alvarez, S., Universitat de Barcelona, 1993.

Theoretical Study of the Reactions of H+H_2 and Its Isotopic Variants Inter- and Intramolecular Isotope Effect

Ju-Beom Song

Department of Chemical Education, Kyungpook National University, 1370 Sankyuk-Dong, Pook-Ku, Taegu 702-701, Korea
Received January 11, 1998

Quasiclassical trajectory calculations were carried out for the reactions of H+H_2 (v=0, J=0) and its isotope variants on the Siegbahn-Liu-Truhlar-Horowitz potential energy surface for the relative energies E between 6 and 150 kcal/mol. The goal of the work was to understand the inter- and intramolecular isotope effects. We examine the relative motion of reactants during the collision using the method of analysis that monitors the intermolecular properties (internuclear distances, geometry of reactants, and final product). As in other works, we find that the heavier the incoming atom is, the greater the reaction cross section is at the same collision energy. Using the method of analysis we prove that the intermolecular isotope effect is contributed mainly by differences in reorientation due to the different reduced masses. We show that above E=30 kcal/mol recrossing also contributes to the intermolecular isotope effect. For the intramolecular isotope effect in the reactions of H+HD and T+HD, we reach the same conclusions as in the systems of O(^{3}P)+HD, F+HD, and Cl+HD. That is, the intramolecular isotope effect below E=150 kcal/mol is contributed by reorientation, recrossing, and knockout type reactions.

Introduction

Recently, we have carried out a series of quasiclassical trajectory (QCT) computations[1-10] for gas phase exchange reactions such as

$$X+H_2 \rightarrow XH+H, \quad (1)$$
$$X+HD \rightarrow XH+D, \quad (2a)$$
$$\rightarrow XD+H, \quad (2b)$$

where X is O(^{3}P), F, Cl, T, and H, in order to understand the effect of translational, vibrational, and rotational energy in the reactants on the reactive cross section. For all of the systems we have studied there is a barrier to reaction which is lowest in the linear configuration and which grows as the X-H-H angle is bent. We have also examined the inter- and intramolecular isotope effects in some of these reactions. In the QCT works certain intermolecular properties (bond

length of H_2 and HD, r; the angle between H_2 or HD and XH, γ; and the final product channel) were monitored at various R values (where R is the shorter of the two XH distances) during the collision. (These coordinates are shown in Figure 1) Our earlier papers[1-10] have proved that this method of analysis is very useful to understand the reaction mechanism and intramolecular isotope effects in reactions (1) and (2). The goal of this work is to understand the inter- and intramolecular isotope effects in the reactions of $H+H_2$ and its isotopic variants using this method. In our earlier paper[9] we tried to understand the inter- and intramolecular isotope effects in the reactions at high energies using the pairwise energy model (PEM) and we could expect any reaction of H_2 and isotopic variants to obey PEM at sufficiently high energy. However, the PEM fails to explain isotope effects at lower energies. To study what causes this failure can give considerable insight into the reaction dynamics.

The question is what causes the inter- and intramolecular isotope effects in the reactions. If the relative motion of the reagent molecule or atom as reactants come together is not different in the isotopic variant reactions, one could not expect any inter- and intramolecular isotope effects in the reactions which have the steric requirement to form the product. Thus, in order to describe the inter- and intramolecular isotope effects in the reactions one must understand the relative motions of reactants during the trajectory. Although the potential energy surface (PES) as a function of three internuclear distances are invariant for reagent isotopic substitution under the Born-Oppenheimer approximations, there are lots of factors which can affect the relative motion of reactants during the collision. First, the skew angle in the skewed coordinate systems that diagonalize the kinetic energy is no longer isotopically invariant. Second, the radial velocity is different for the different isotopes since the reduced masses of reactants are changed by the isotopic substitution. Third, if the center of mass of the reagent molecule is shifted to the heavier isotope atom from the center of charge for isotopic substitution, the potential $V(R_{CM},\chi)$[11-14] is not symmetric any more with respect to the center of mass. Here R_{CM} is the distance from the incoming atom to the center of mass of the reagent molecule and χ is the angle between R_{CM} and the molecule axis. Fourth, if the center of mass is shifted to the heavier isotope atom from the center of charge for the isotopic substitution and there is interaction between two reactants, the interaction acts differently[12] on the relative motion of the molecule for the attack of the incoming atom to two isotope atom ends during the collision. Fifth, when the reagent molecule vibrates, its vibrating length, velocity, and period may change isotopically. We already interpreted the intramolecular isotope effect in the reactions of $O(^3P)$+HD,[1] F+HD,[5] and Cl+HD[10] in terms of these five factors. We will take a trip to interpret how the five factors given above affect the relative motions of reactants and then how the variation of the relative motions affects the inter- and intramolecular isotope effects in the reactions.

The reaction of $H+H_2$ and its isotopic variants are the prototypes of gas 'phase bimolecular reactions. The experimental and theoretical works has been reviewed several times[15-17] and a number of important dynamics[18-57] studies have been made for these reactions in recent years.

In the present paper, we confine our study only to the reactions which have the same reagent molecule in order to understand the intermolecular isotope effect, that is,

$$Y+H_2 \rightarrow YH+H, \tag{3}$$

where Y is H or an isotope of H. And in order to understand the intramolecular isotope effect, we treat the two reactions; H+HD (υ=0, J=0) and T+HD (υ=0, J=0), where υ and J are the vibrational and rotational quantum numbers, respectively.

$$Y+HD \rightarrow YH+D, \tag{4a}$$
$$\rightarrow YD+H, \tag{4b}$$

where Y is H or T. We will try to separate the effects of the five factors on the inter- and intramolecular isotope effects in the reactions as much as possible.

Theory

The potential energy surface used in this work was the accurate Siegbahn-Liu-Truhlar-Horowitz (SLTH) surface.[58] The QCT calculations were carried out as described in our earlier papers[1-5] using the VENUS program developed by Hase and coworkers.[59] The program monitors three internuclear distances throughout the trajectory. If the distance from the incoming atom to one atom of the reagent molecule reaches, say, 1.4 Å before the distance from the incoming atom to the other atom of the reagent molecule does, we say the incoming atom hits the former atom at R= 1.4 Å. The process is then repeated at other R such as 1.2 and 0.93 Å. The latter distance, $R^{\dagger}$, corresponds to the linear transition state. We expect collisions which reach this distance to react. At each value of R we also determine r and γ. Finally we keep track of which diatomic product is formed at the end of each trajectory. At the end we determine the average values of r and γ as well as the cross sections for the incoming atom hitting the one and the other atom of reagent molecule at particular R value.

The total cross section for collisions where the distance from the incoming atom to the one atom of the molecule reaches first $R^{\dagger}$ is defined as $Q^{\dagger}_{hit}$. Collisions that reach $R^{\dagger}$ are divided into reactive collisions and nonreactive collisions; the latter are called "recrossing" collisions. Reactive collisions are divided into two groups; direct reactions, where the incoming atom first reaches the one atom of the molecule at $R^{\dagger}$ and catches the atom, and knockout reactions, where the incoming atom first reaches the one atom of the molecule at $R^{\dagger}$ but catches the other atom.

In this paper the reaction probability, P_R, is defined by

$$P_R = \frac{Q_R}{Q^{\dagger}_{hit}} \tag{5}$$

Here Q_R is the reactive cross section for forming product. We determine the intramolecular isotope effect, I_R, for reactions Y+HD where Y is H or T by

$$I_R(Y) = \frac{Q_R(YD)}{Q_R(YH)} \tag{6}$$

Here Q_R(YD) and Q_R(YH) are reaction cross sections for YD and YH products, respectively. The intermolecular iso-

tope effect, I_T, for the reaction Y+H_2 (Y is an isotope of H) is defined by

$$I_T(Y) = \frac{Q_R(Y-H_2)}{Q_R(H-H_2)} \quad (7)$$

Here Q_R(Y-H_2) and Q_R(H-H_2) are reaction cross sections for YH and H_2 products in the reaction of Y+H_2 and H+H_2, respectively.

Standard Monte Carlo sampling procedure were used to select the initial conditions for each trajectory. In most cases 7,000 trajectories were run with varying a maximum impact parameter from 0.7 Å to 1.8 Å.

Results and Discussions

The intermolecular isotope effect in the reaction Y+H_2 (υ=0, J=0) (Y is H or an isotope of H). To better understand the intermolecular isotope effect in the reaction of Y+H_2, where we have used the masses of 1(H), 3(T), and 20(X) amu for the mass of the Y atom (X is a ficticious hydrogen isotope atom), it is necessary to examine the PES. We follow the approach of Loesch[11] and Levine and coworkers[12-14] by plotting potential energy contours for fixed r as a function of R_{CM} and χ. (See Fig. 1) Our work will demonstrate, however, that the H_2 bond length is considerably elongated by the time the approaching atom reaches the distance $R^\dagger$. We show in Figure 2 plots of the potential contours $V(R_{CM}, \chi)$ for $r=r_e$=0.7414, 0.83, 0.93, and 1.0 Å (where r_e is the equilibrium bond length of H_2). The third one, $r^\dagger$, is the H_2 distance at the linear transition state. The plot for $r=r_e$, 0.941, and 1.046 Å were also shown in Refs. 29 and 12. In each case $R_{CM}=\infty$ corresponds to the zero of energy. At $r=r_e$, the potential is nearly independent of χ, but as r increases it becomes oblate and it is remarkably oblate[12-14] at $r=r^\dagger$. (An oblate potential is lower for the collinear configuration than for the perpendicular configuration.) The potential contours are quite similar near χ=90° for all four values of r. This indicates that the barrier to rotate for a particular value of R_{CM} is approximately independent of r. Figure 2 also shows the location of the potential barrier which separates the reactant and the product sides of the surface. Each point on this curve was determined by fixing r and χ, plotting the potential against R_{CM} and locating the maximum (if it exists). The product region is centered at χ=180°, its angular width

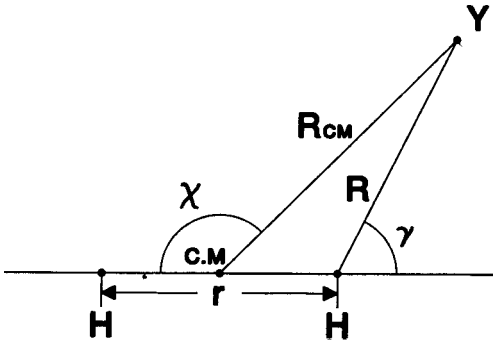

Figure 1. Various coordinates for a collision of Y+H_2.

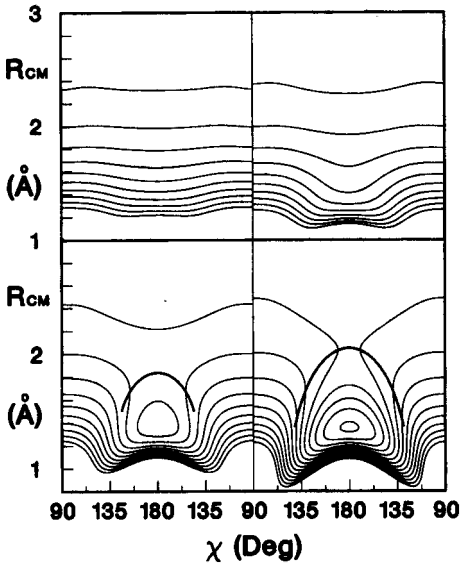

Figure 2. Potential energy contours for the system Y+H_2 plotted for the Jacobi coordinates R_{CM} and χ defined in Figure 1. χ=180° corresponds to linear Y-H-H. The four plots correspond to r= 0.7414 (upper left), 0.83 (upper right), 0.93 (lower left), and 1.0 Å (lower right). In each plot the zero-of-energy, V=0 corresponds to $r=r$ and $R_{CM}=\infty$. The uppermost contour in all plots has the value V=1 kcal/mol. Successive contours in all plots are 2 kcal/mol higher and the bottom contour has the value V=19 kcal/mol. The heavy curve in each plot gives the location of the potential barrier, computed as described in the text, which separates the reactant (large R_{CM}) and product (small R_{CM}) regions of the surface.

becomes much broader as r increases. We also observe fairly deep well in the surface for r=1.0 Å. This is located in the product region where the YH molecule is forming. As r increases the open angle of the cone of acceptance with respect to χ becomes wider.

Figure 3 shows the reaction cross sections as a function of relative collision energy, E, for reactions of Y+H_2 (υ=0, J=0) (where Y is H, T, and X with the mass of 20 amu, and υ and J are the vibrational and rotational quantum numbers, respectively.) below E=100 kcal/mol. These results agree well with the previous studies[60] on the same PES. The thresholds for three reactions are in range of 6.5-6.9 kcal/mol. The heavier the incoming atom is, the lower is the threshold in the reaction. General behaviors of reaction cross sections are similar in the three reactions but the reaction cross sections become larger as the incoming atom becomes heavier. In other words, the heavier incoming atom is more reactive than the lighter atom in an entire range of collision energy. Figure 4 shows the intermolecular isotope effects, I_T(T) and I_T(X), defined in Eq. (7). Both I_T (T) and I_T(X) start from infinite near threshold, fall down rapidly, reach minima at E=30 kcal/mol and then increase very slowly. It is necessary to understand thresholds of three reactions before we discuss I_T. Mayne[60] explained the thresholds in terms of the skew angle and vibrational zero-point energy (ZPE) of H_2 molecule. The values of skew angle for linear configuration are 60°, 52°, and 46° for Y=H, T, and X, respectively. Mayne[60] suggested that reaction at threshold is enhanced by a reduction of the skew angle, *i.e.*,

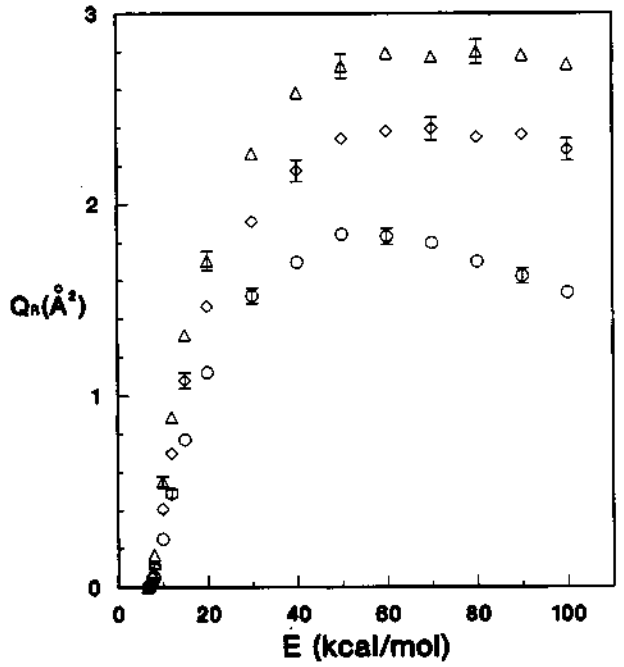

Figure 3. Reaction cross section for Y+H_2 (υ=0, J=0)⟶YH+H as a function of relative collision energy below 100 kcal/mol. Circles, diamonds, and triangles correspond to Y=H, T, and X=20 amu, respectively. The 68% confidence limits are shown selectively.

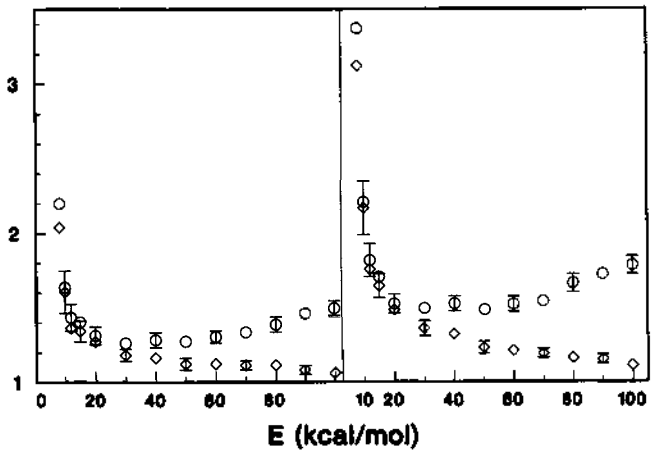

Figure 4. Intermolecular isotope effects, I_T, defined in Eq. 7 and reorientation effects on I_T in the reaction of Y+H_2 (υ=0, J=0)⟶YH+H as a function of relative collision energy below 100 kcal/mol. The left panel shows $I_T(T)=Q_R(T+H_2)/Q_R(H+H_2)$ and the right panel shows $I_T(X)=Q_R(X+H_2)/Q_R(H+H_2)$ where X is a fictitious hydrogen isotope atom with 20 amu. Circles and diamonds correspond to I_T and reorientation effect, respectively. The gap between diamond and circles at each collision energy corresponds to the recrossing effect on I_T.

more vibrational ZPE is available for crossing the barrier to reaction at smaller skew angles for this particular PES. However, in our calculations for three reactions of Y+H_2 (υ = − 1/2, J=0) (that is, there is no ZPE) we obtained the same order of thresholds. Thus, Mayne's explanation may not be reliable in this case. To get the lowest threshold in some reaction, it is necessary for the reaction to follow the minimum energy path on the PES. Yet we can never expect the system to follow the minimum energy path. We would expect only that the system follows it as closely as possible. In order for this to happen, the radial velocity of the incoming atom must be as slow as possible. The reduced masses in three reactions are $\mu_{H,H}$=0.67, $\mu_{T,H}$=1.81, $\mu_{X,H}$=2.75 amu. At a given collision energy, the relative radial velocities for the incoming atoms H, T, and X are in the ratio 1 : 0.74 : 0.6. As the incoming atom becomes heavier the trajectory can follow the minimum energy path more closely. In terms of traditional "mass weighted coordinates" description, as the incoming atom becomes heavier the skew angle becomes smaller but the product valley becomes remarkably wider. Thus, the translational energy can be used more efficiently to overcome the barrier for the broad product valley than for the narrow product valley. In addition, according to Mayne' suggestion,[60] it may be true that the vibrational ZPE is more efficient to cross the barrier for the heavier incoming atom. However, it may not be due to the smaller skew angle but due to the slower radial velocity of the heavier incoming atom.

Now we get back to discuss the intermolecular isotope effect. Mayne suggested that I_T is caused only because the molecule has more time to reorient toward favorable alignment for the heavier incoming atom due to the heavier reduced mass. We agree with Mayne's explanation and prove it as follows. Table 1 shows the average values of γ (see Fig. 1) and the average values of bond length of H_2, $\langle r\rangle_n$ for reactive trajectories at various R in three reactions at E=10 kcal/mol. In all three isotope cases the average values of the bond length of H_2 for reactive trajectories and total trajectories increase dramatically from $\langle r\rangle_n$=0.77 Å at R=1.7 Å to $\langle r\rangle_n$=1.03 Å at R=0.93 Å. At this low collision energy $\langle r\rangle_n$ is little influenced by the isotopic substitution

Table 1. Properties of collision of Y+H_2 (υ=0, J=0) at E=10 kcal/mol[a]

Y	R=1.7 Å	1.5 Å	1.3 Å	1.1 Å	1.0 Å	0.93 Å
			$\langle r\rangle_{all}$ (Å)[b]			
H	0.773	0.786	0.817	0.881	0.948	1.020
T	0.780	0.785	0.816	0.869	0.949	1.033
X[c]	0.776	0.794	0.812	0.882	0.963	1.034
			$\langle r\rangle_n$ (Å)[d]			
H	0.766	0.788	0.799	0.858	0.958	1.023
T	0.779	0.770	0.810	0.857	0.950	1.032
X	0.778	0.779	0.803	0.867	0.964	1.034
			$\langle\gamma\rangle_n$ (degree)[e]			
H	28.3	28.5	28.1	25.5	22.5	20.3
T	33.4	33.1	32.2	24.4	19.1	18.2
X	37.3	36.6	34.1	22.3	17.2	16.0

[a] A total of 7,000 quasiclassical trajectories were computed with a maximum impact parameter b_{max}=1.8 Å. [b] The average value of the H-H bond length r for all trajectories which reach a given Y-H bond length R. [c] The X is a fictitious hydrogen isotope atom with the mass of 20 amu. [d] The average value of r for all reactive trajectories at R. [e] The average value of the Y-H-H bond γ angle for all reactive trajectories at R. Linear Y-H-H corresponds to γ= 0°.

for the incoming atom. One can know easily that the potential $V(R_{CM}, \chi)$ changes from nearly χ-independent type into strongly oblate as the incoming atom approaches the H_2 molecule, by comparing $<r>$ at each R with Figure 2. The oblate type potential tends to reorient[11-14] the trajectory into the collinear during the collision. The average values of γ, $<\gamma>_r$, for only reactive trajectories in Table 1 decrease as the collision progresses. The decrease in $<\gamma>_r$ during the collision is more serious for the heavier incoming atom than for the lighter one. For example, $<\gamma>_r$ is reduced by 8° for the incoming H atom but it is reduced by 21.3° for the incoming X atom as the value of R decreases from 1.7 to 0.93 Å. As discussed by other authors,[11-14] this is due to the fact that the H_2 molecule has more time to reorient itself towards favorable orientation for the heavier incoming atom than for the lighter one on the oblate potential energy surface. The reorientation contribution to I_T is shown in Figure 4 (in diamonds). The reorientation contribution is reduced considerably as the collision energy increases. Below E=30 kcal/mol I_T is influenced mainly by the reorientation, but above E=30 kcal/mol I_T starts to be affected considerably by the other factor ("recrossing") which contributes to I_T by the gaps between circles and diamonds in Figure 4. We determined the reaction probability P_R, defined in Eq. (5), as a function of relative collision energy for three reactions shown in Figure 5. Around threshold P_R is unity or near unity in all three reactions. But, as the collision energy increases, P_R decreases more seriously for the lighter incoming atom. In order to understand the behaviors of P_R in the three isotope reactions we determined the average values of the bond length of H_2 for all trajectories which reach each R, $<r>_{all}$, at E=50 and 100 kcal/mol as shown in Table 2. Unlike E=10 kcal/mol at which $<r>_{all}$ at each R is very close to each other in the three reactions, $<r>_{all}$ at each

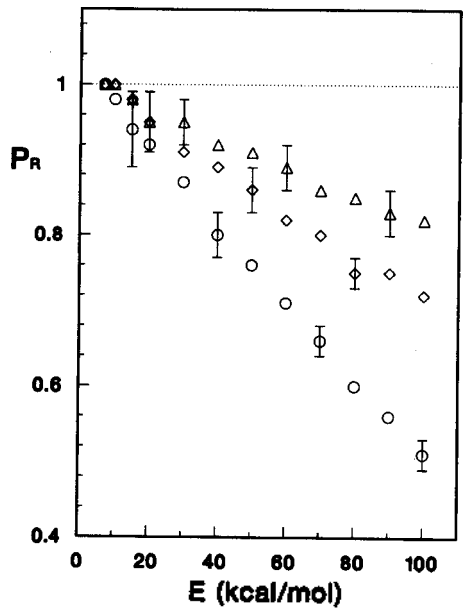

Figure 5. Reaction probability, P_R, defined in Eq. 5 plotted against the relative collision energy below 100 kcal/mol for Y+H_2 (υ=0, J=0)→YH+H. Circles, diamonds, and triangles correspond to Y=H, T, and X=20 amu, respectively. The 68% confidence limits are shown selectively.

Table 2. Aaverage bond length of H_2 in collisions of Y+H_2 (υ=0, J=0) at E=50 and 100 kcal/mol[a]

Y	R=1.7 Å	1.5 Å	1.3 Å	1.1 Å	1.0 Å	0.93 Å
			E=50 kcal/mol			
H	0.769	0.774	0.785	0.809	0.833	0.894
T	0.771	0.775	0.784	0.814	0.852	0.919
X[b]	0.772	0.778	0.785	0.814	0.856	0.936
			E=100 kcal/mol			
H	0.768	0.770	0.777	0.792	0.803	0.816
T	0.768	0.773	0.781	0.800	0.814	0.873
X	0.769	0.776	0.785	0.801	0.819	0.906

[a] A total of 7,000 quasiclassical trajectories were computed with a maximum impact parameter b_{max}=1.8 Å. The entry is the average value of the H-H bond length r for all trajectories which reach a given Y-H bond length R. [b] The X is a fictitious hydrogen isotope atom with the mass of 20 amu.

R is shorter for the lighter incoming atom than for the heavier one at E=50 and 100 kcal/mol, in particular near the transition state. The differences between $<r>_{all}$ in H+H_2, and in X+H_2 at R=R‡=0.93 Å are 0.02, 0.042, and 0.109 Å at E= 10, 50, and 100 kcal/mol, respectively. That is, they become larger with increase in the relative collision energy. In our opinion, those differences of $<r>_{all}$ at R=R‡ mainly cause the tremendous differences of reaction probabilities in three reactions, even though there is possibility that the smaller skew angle albeit the broader exit valley in the heavier incoming isotope atom gives the high reaction probability.

The intramolecular isotope effect in reactions H (T)+HD (υ=0, J=0). To better understand reactions H (T)+HD (υ=0, J=0) it is useful to examine PES for fixed r as a function of R_{CM} and χ (see Fig. 6) for the isotope substitution. We show in Figure 7 plots for H+HD of the potential contours $V(R_{CM}, \chi)$ for r=0.7414 and 0.923 Å. Kornweitz *et al.*[14] showed analytically how the shift of the center of mass of molecule from the center of charge due to the isotopic atom affects the potential contours. The potential contours are always recessed more from the barrier region for the heavier isotopic atom end. In addition, the open angle of the cone of acceptance with respect to χ is wider in the heavier atom than in the lighter atom.

Figure 8 shows the reaction cross sections as a function of relative collision energy in reactions H+HD (υ=0, J=0)[31,61-65] and T+HD (υ=0, J=0).[66,67] The total reaction cross

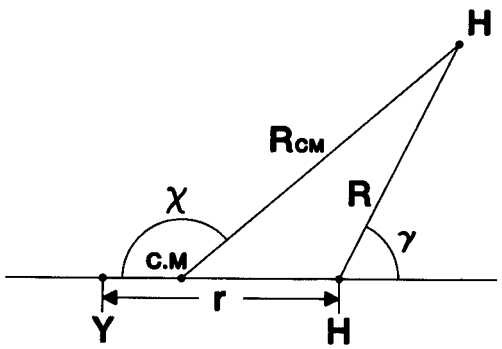

Figure 6. Various coordinates for a collision of H+HY.

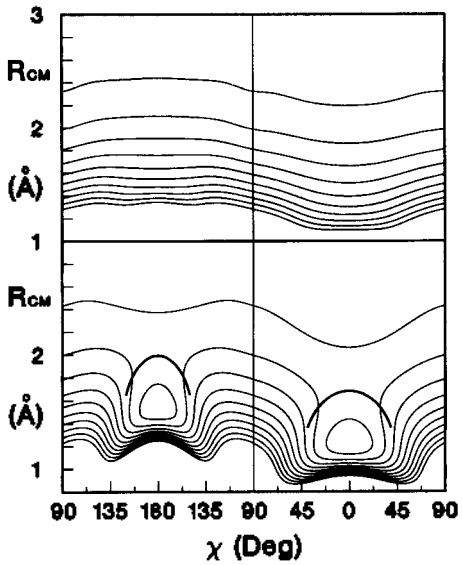

Figure 7. Potential energy contours for the system H+HD plotted for the Jacobi coordinates R_{CM} and χ defined in Fig. 6. χ=0° and χ=180° correspond to linear H-D-H and H-H-D, respectively. The two plots correspond to r=0.7414 Å for the top panel and 0.93 Å for the bottom panel. The others are explained in the footnote of Fig. 2.

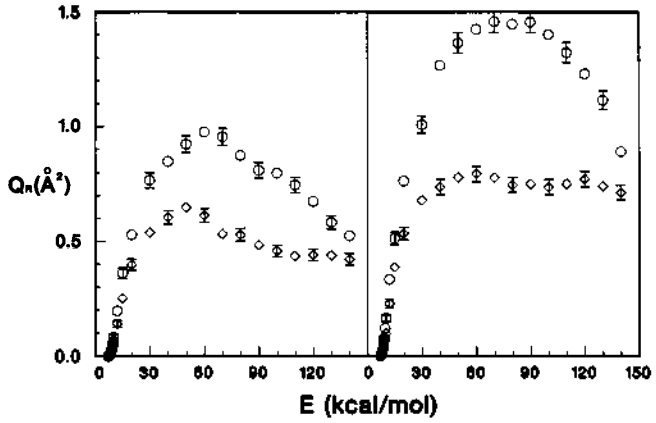

Figure 8. Reaction cross sections for H+HD (υ=0, J=0) (left panel) and T+HD (υ=0, J=0) (right panel) plotted against the relative collision energy below 150 kcal/mol. In both panels circles and diamonds correspond to HD(TD) and H_2(TH), respectively. The 68% confidence limits are shown alternatively.

section (the sum of reaction cross sections for TH and TD) in reaction T+HD is always bigger than that in reaction H+HD at the same collision energy. This intermolecular isotope effect can be described by the similar explanation discussed for the reactions (3). In both reactions the lighter atom H of the HD molecule is preferentially abstracted near threshold. This phenomenon was also seen for reactions of $O(^3P)$+HD,[1] F+HD,[5] and Cl+HD.[10] In reaction of Cl+HD (υ=0, J=0)[10] we showed that the fact that the lighter H atom is preferentially abstracted near threshold is due to the vibrational zero-point energy (ZPE) of the reagent that near threshold dominates the other several factors which make the heavier D atom be preferentially abstracted. This argument is also pertinent in reactions of H(T)+HD. (If the

Table 3. The average value of the bond angle γ for all reactive trajectories at each R in collisions of H+HD (υ=0, J=0) and T+HD (υ=0, J=0) at E=12 kcal/mol[a]

System	R=1.7 Å	1.5 Å	1.3 Å	1.1 Å	0.93 Å
H+HD	27.4	27.4	27.4	27.5	25.7
	32.1	31.7	30.9	28.7	23.3
T+HD	32.5	33.1	34.0	31.7	23.0
	38.6	37.6	35.3	27.7	20.1

[a] A total of 7,000 quasiclassical trajectories were computed with a maximum impact parameter b_{max}=1.8 Å. In each system the upper entry refers to the average value of the H-H-D or T-H-D bond angle γ for all reactive trajectories at R and the lower entry refers to the average value of the H-D-H or T-D-H angle γ for all reactive trajectories at R. Linear H-H-D and H-D-H or T-H-D and T-D-H correspond to γ=0°. The unit of entry is degree.

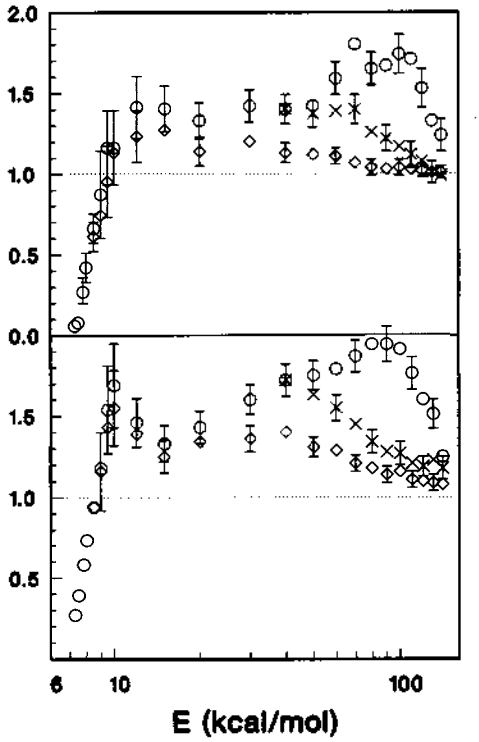

Figure 9. Intramolecular isotope effects, I_R, defined in Eq. 6 and the effects of various factors on I_R for H+HD (υ=0, J=0) (upper panel) and T+HD (υ=0, J=0) (lower panel) plotted against the relative collision energy below 150 kcal/mol. In both panels circles and diamonds represent I_R and the reorientation effect, respectively. Below E=40 kcal/mol the gap between cross and diamond at each collision energy denotes the recrossing effect. Above E=50 kcal/mol the gap between cross and diamond at each collision energy corresponds to the recrossing effect and the gap between circle and cross corresponds to the effect of the knockout reaction on I_R. The 68% confidence limits are shown selectively.

ZPE is assumed to be zero in reactions of H(T)+HD, the heavier D atom is always preferentially abstracted, even near threshold.) Well above threshold, the incoming atom favors the heavier D atom over the lighter H atom. Several factors that make the incoming atom favor the heavier atom over the lighter H atom at energies well above threshold

have been proposed by Levine and coworkers[12-14] and our earlier works.[1,5,10] The first factor is the potential $V(R_{CM}, \chi)$ difference between in the heavier atom D end and in the lighter atom H end due to the shift of the center of mass from the center of charge of the HD molecule to near the D end. Second, the repulsive potential between the incoming atom and the HD molecule for the oblique approach of the incoming atom to the HD molecule. Third, the "recrossing", that is, the trajectory crosses the activation barrier but gets back into the reactant channel. Fourth, the knockout reactions where the incoming atom first hits H(D) but reacts with D(H). Here, the first two factors are considered as the "reorientation" effect. The relative importance of reorientation effect is shown nicely in Table 3 that shows the average values $\langle\gamma\rangle_r$ for reactive collisions at various values of R in the reactions of H+HD and T+HD at E=12 kcal/mol. For the reaction of H+HD, as the incoming H atom approaches the H end of HD molecule from R=1.7 to 0.93 Å, $\langle\gamma\rangle_r$ is nearly constant at around 27°, whereas it is reduced by some 9° as the incoming H atom approaches the D end. And in the reaction of T+HD, as the incoming T atom approaches the H end from R=1.7 to 0.93 Å $\langle\gamma\rangle_r$ is decreased by 9.5° but it is decreased by 18.5° when the T atom progresses to the D end. Thus, $\langle\gamma\rangle_r$ decreases much more for the approaching of the incoming atom to the D end of HD molecule than to the H end. This causes the reorientation effect which contributes mainly to I_R at low collision energy. In the present paper we have tried to separate them in order to see how much each factor contributes to the intramolecular isotope effect, I_R. The results are shown in Figure 9. In Figure 9, the gap between cross and diamond at each collision energy denotes the recrossing effect below E=40 kcal/mol, the gap between cross and diamond at each collision energy corresponds to the recrossing effect, and the gap between circle and cross corresponds to the effect of the knockout reaction on I_R above E=50 kcal/mol. In both reactions I_R starts from zero, continues to increase with increase in relative collision energy, reaches a maximum around E=80 kcal/mol, and then decrease rapidly. Yet, I_R is always somewhat smaller in reaction of H+HD than in reaction of T+HD at the same collision energy. As shown in Figure 9 and Table 3, this is mainly due to the difference in reorientation effect between the two reactants. That is, the reorientation effect is relatively smaller in reaction of H+HD than in reaction of T+HD, because the H atom approaches the HD molecule faster than the T atom does. In both reactions the effect of recrossing on I_R increases as the collision energy increases. The effect of recrossing on I_R in reaction of H+HD is relatively more important than that of reorientation, whereas the reverse is true in reaction of T+HD below E=50 kcal/mol. In both reactions the knockout reaction starts to contribute to I_R at E=50 kcal/mol and it is a primary factor which causes $I_R > 1$ around E=100 kcal/mol.

Conclusions

We carried out the QCT calculations for the reaction of $H+H_2$ and its isotope variants in order to understand the inter- and intramolecular isotope effects at low collision energy ($E \leq 100$ kcal/mol). Our work confirms that the intermolecular isotope effect in the reactions of $Y+H_2$ (where Y is H or its isotope atom) is caused mainly by reorientation effect below E=30 kcal/mol. Above E=30 kcal/mol the recrossing contributes to the intermolecular isotope effect. In addition, we concluded that the lower threshold energies for the reactions with the heavier incoming atom is not due to the vibrational zero-point energy but due to the slower radial velocity because of the heavier reduced mass. For the reactions at high energies, the intermolecular isotope effect is explained by the pairwise energy model. For the intramolecular isotope effect in the reactions of H+HD and T+HD, we reached the same conclusions as in the systems $O(^3P)$+HD, F+HD, and Cl+HD. That is, the intramolecular isotope effect below E=100 kcal/mol is contributed by reorientation, recrossing, and knockout type reactions.

Acknowledgment. The authors acknowledge W. L. Hase for making trajectory program VENUS available to us. A considerable grant of computer time from the UIC computer center is gratefully acknowledged. This work is supported partly by Kyungpook National University Fund. Finally, it is a pleasure to thank Eric A. Gislason for very helpful discussions and advices.

References

1. Song, J. B.; Gislason, E. A. *J. Chem. Phys.* **1993**, *99*, 5117.
2. Song, J. B.; Gislason, E. A.; Sizun, M. *J. Chem. Phys.* **1995**, *102*, 4885.
3. Song, J. B.; Gislason, E. A. *J. Chem. Phys.* **1995**, *103*, 8884.
4. Song, J. B.; Gislason, E. A. *J. Phys. Chem.* **1996**, *100*, 195.
5. Song, J. B.; Gislason, E. A. *J. Chem. Phys.* **1996**, *104*, 5834.
6. Song, J. B.; Gislason, E. A. *Chem. Phys.* **1996**, *202*, 1.
7. Song, J. B.; Gislason, E. A. *Chem. Phys.* **1996**, *212*, 259.
8. Song, J. B.; Gislason, E. A. *J. Chem. Phys.* **1996**, *105*, 10429.
9. Song, J. B.; Gislason, E. A. *J. Chem. Phys.* **1997**, *214*, 23.
10. Song, J. B.; Gislason, E. A. *Chem. Phys.* (accepted).
11. Loesch, H. *J. Chem. Phys.* **1986**, *104*, 213; **1987**, *112*, 85.
12. Levine, R. D. *J. Phys. Chem.* **1990**, *94*, 8872.
13. Johnston, G. W.; Kornweitz, H.; Schechter, I.; Persky, A.; Katz, R.; Bersohn, R.; Levine, R. D. *J. Chem. Phys.* **1991**, *94*, 2749.
14. Kornweitz, H.; Persky, A.; Levine, R. D. *J. Phys. Chem.* **1991**, *95*, 1621.
15. (a) Truhlar, D. G.; Wyatt, R. E. *Annu. Rev. Phys. Chem.* **1976**, *27*, 1. (b) *Adv. Chem. Phys.* **1977**, *36*, 141.
16. (a) Schatz, G. C. In *The Theory of Chemical Reaction dynamics*; Clary, D. C., Ed.; Reidel: Dordrecht, 1986; p 1. (b) *Annu. Rev. Phys. Chem.* **1988**, *39*, 317.
17. Valentini, J. J.; Philips, D. L. In *Biomolecular collisions*; Ashfold, M. N. R.; Baggott, J. E., Ed.; Royal Society: London, 1989; p 1.
18. Nieh, J. C.; Valentini, J. J. *Phys. Rev. Lett.* **1988**, *60*, 519.

19. Philips, D. L.; Levene, H. B.; Valentini, J. J. *J. Chem. Phys.* **1989**, *90*, 1600.
20. Valentini, J. J.; Philips, D. L. In *Advances in Gas Phase Photochemistry and kinetics*; Ashfold, M. N. R.; Baggott, J. E., Ed; Royal Society of Chemistry: London, 1989; Vol. 2.
21. Rinnen, K. D.; Kliner, D. A. V.; Zare, R. N. *J. Chem. Phys.* **1989**, *91*, 7514.
22. Kliner, D. A. V.; Rinnen, K. D.; Zare, R. N. *Chem. Phys. Lett.* **1990**, *166*, 107.
23. Kliner, D. A. V.; Zare, R. N. *J. Chem. Phys.* **1990**, *93*, 2107.
24. Buntin, S. A.; Giese, C. F.; Gentry, W. R. *Chem. Phys. Lett.* **1990**, *168*, 513.
25. Sinha, A.; Hsiao, M. C.; Crim, F. F. *J. Chem. Phys.* **1991**, *94*, 4928.
26. Hillenbrand, E. A.; Main, D. J.; Jorgensen, A. D.; Gislason, E. A. *J. Phys. Chem.* **1984**, *88*, 1358.
27. Riederer, D. E.; Jorgensen, A. D.; Gislason, E. A. *J. Chem. Phys.* **1991**, *94*, 5980.
28. Muga, J. G.; Levine, R. D. *J. Chem. Soc., Faraday Trans.* **1990**, *86*, 1669.
29. Hernandez, R.; Miller, W. H. *Chem. Phys. Lett.* **1993**, *214*, 129.
30. Sathyamurthy, N.; Toennies, J. P. *Chem. Phys. Lett.* **1988**, *143*, 323.
31. Mayne, H. R. *J. Phys. Chem.* **1988**, *92*, 6289.
32. Aoiz, F. J.; Herrero, V. J.; Saez Ravanos, V. *Chem. Phys. Lett.* **1989**, *161*, 270.
33. Aoiz, F. J.; Candela, V.; Herrero, V. J.; Saez Ravanos, V. *Chem. Phys. Lett.* **1990**, *169*, 243.
34. Dove, J. E.; Mandy, M. E.; Mohan, V.; Sathyamurthy, N. *J. Chem. Phys.* **1990**, *92*, 7373.
35. Mayne, H. R. *J. Am. Chem. Soc.* **1990**, *112*, 8165.
36. Aoiz, F. J.; Herrero, V. J.; Saez Ravanos, V. *J. Chem. Phys.* **1991**, *94*, 7991.
37. (a) Mladenovic, M.; Zhao, M.; Truhlar, D. G.; Schwenke, D. W.; Sun, Y.; Kouri, D. J. *Chem. Phys. Lett.* **1988**, *146*, 358. (b) *J. Phys. Chem.* **1988**, *92*, 7035. (c) Zhao, M.; Truhlar, D. G.; Kouri, D. J.; Sun, Y.; Schwenke, D. W. *Chem. Phys. Lett.* **1989**, *156*, 281.
38. Zhang, J. Z. H.; Miller, W. H. *Chem. Phys. Lett.* **1988**, *153*, 465; **1989**, *159*, 130. (b) *J. Chem. Phys.* **1989**, *91*, 1528.
39. Manolopoulos, D. E.; Wyatt, R. E. *Chem. Phys. Lett.* **1989**, *159*, 123.
40. Pack, R. T.; Parker, G. A. *J. Chem. Phys.* **1989**, *90*, 3511.
41. Park, T. J.; Light, J. C. J. Chem. Phys. 1989, 91, 974.
42. (a) Blais, N. C.; Zhao, M.; Mladenovic, M.; Truhlar, D. G.; Schwenke, D. W.; Sun, Y.; Kouri, D. J. *J. Chem. Phys.* **1989**, *91*, 1038. (b) Blais, N. C.; Zhao, M.; Truhlar, D. G.; Schwenke, D. W.; Kouri, D. J. *Chem. Phys. Lett.* **1990**, *166*, 11. (c) Zhao, M.; Truhlar, D. G.; Blais, N. C.; Schwenke, D. W.; Kouri, D. J. *J. Phys. Chem.* **1990**, *94*, 6696; **1990**, *94*, 7074.
43. Kress, J. D.; Bacic, Z.; Parker, G. A.; Pack, R. T. *J. Phys. Chem.* **1990**, *94*, 8055.
44. Miller, W. H. *Annu. Rev. Phys. Chem.* **1990**, *41*, 245.
45. Continetti, R. E.; Zhang, J. Z. H.; Miller, W. H. *J. Chem. Phys.* **1990**, *93*, 5356.
46. Auerbach, S. M.; Zhang, J. Z. H.; Miller, W. H. *J. Chem. Soc., Faraday Trans.* **1990**, *86*, 1701.
47. Miller, W. H.; Zhang, J. Z. H. *J. Phys. Chem.* **1991**, *95*, 12.
48. (a) Auerbach, S. M.; Miller, W. H. *J. Chem. Phys.* **1993**, *98*, 6917. (b) Manthe, U.; Miller, W. H. *J. Chem. Phys.* **1993**, *99*, 3411.
49. Thompson, W. H.; Miller, W. H. *Chem. Phys. Lett.* **1993**, *206*, 123.
50. Auerbach, S. M.; Miller, W. H. *J. Chem. Phys.* **1994**, *100*, 1103.
51. Shin, S.; Light, J. C. *J. Chem. Phys.* **1994**, *101*, 2836.
52. Aoiz, F. J.; Banares, L.; D'Mello, M. J.; Herrero, V. J.; Saez Rabanos, V.; Schnieder, L.; Wyatt, R. E. *J. Chem. Phys.* **1994**, *101*, 5781.
53. Miller, W. H. In *Methods in Computational Molecular Physics*; Wilson, S.; Diercksen, G. H. F., Ed.; Plenum: New York, 1992; p 519.
54. Continetti, R. E.; Balko, B. A.; Lee, Y. T. *J. Chem. Phys.* **1990**, *93*, 5719.
55. Continetti, R. E.; Zhang, J. Z. H.; Miller, W. H. *J. Chem. Phys.* **1990**, *93*, 5356.
56. Neuhauser, D.; Judson, R. S.; Kouri, D. J.; Adelman, D. A.; Snafer, N. E.; Kliner, D. A. V.; Zare, R. N. *Science* **1992**, *257*, 519.
57. Kupperman, A.; Wu, Y.-S. M. *Chem. Phys. Lett.* **1993**, *205*, 577.
58. (a) Siegbahn, P.; Liu, B. *J. Chem. Phys.* **1978**, *68*, 2457. (b) Truhlar, D. G.; Horowitz, C. J. *J. Chem. Phys.* **1978**, *68*, 2466; 1979, 71, 1514E.
59. (a) Hase, W. L.; Duchovic, R. J.; Hu, X.; Lim, K. F.; Lu, D. H.; Swamy, K. N.; VandeLinde, S. R.; Wolf, R. J. VENUS (obtained directly from Professor Hase). (b) Hu, X.; Hase, W. L.; Pirraglia, T. *J. Comput. Chem.* **1991**, *12*, 1014.
60. Mayne, H. R. *J. Chem. Phys.* **1980**, *73*, 217.
61. Chou, C. C.; Rowland, F. S. *J. Chem. Phys.* **1967**, *46*, 812.
62. White, J. M. *Chem. Phys. Lett.* **1969**, *4*, 441.
63. Boonenberg, C. A.; Mayne, H. R. *Chem. Phys. Lett.* **1984**, *108*, 67.
64. Schechter, I.; Kosloff, R.; Levine, R. D. *J. Phys. Chem.* **1986**, *90*, 1006.
65. Garrett, B. C.; Truhlar, D. G.; Schatz, G. C. *J. Am. Chem. Soc.* **1986**, *108*, 2876.
66. Garrett, B. C.; Truhlar, D. G.; Grev, R. S.; Walker, R. B. *J. Chem. Phys.* **1980**, *73*, 235.
67. Seewald, D.; Wolfgang, R. *J. Chem. Phys.* **1967**, *46*, 1207.